Title Page Dummy

This Page will be Replaced before Printing

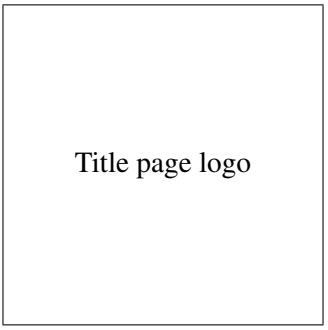

Abstract Dummy Page.

Contents

1 Introduction 5
1.1 Project Purpose and Goal 5
1.2 Previous Work 5

2 Background 6
2.1 Electromagnetic Fields 6
2.1.1 Magnetic Flux and Induction 7
2.2 Series decompositions of the magnetic field 8
2.2.1 Cylindrical Coordinates 8
2.2.2 Bessel Functions 10
2.2.3 Bessel-Fourier-Fourier Series 12
2.2.4 Fundamentals and Harmonics of the BFF Series. 14
2.3 Signal Processing 16
2.3.1 Filters 16
2.3.2 Least Squares Fitting 16

3 The Translating Coil Magnetometer 17
3.1 PCB printed coils 17
3.2 Positional Encoder 17
3.3 Geometric Lidar Measurements 17
3.4 Fast Digital Integrators 17
3.5 The Measurement Assembly 17

4 Measurements 18
4.1 Solenoidal Field Maps 18
4.2 The Magnet-Magnetometer Yaw Angle Peak Shift 18

5 Post Processing 19
5.1 Lidar Scans 19
5.2 Coil Induction Analysis 19
5.3 Bessel-Fourier-Fourier Series Fitting 19
5.4 Estimating the Magnet-Magnetometer Yaw Angle 19

6 Discussion 20
6.1 Metrological Characterization 20
6.2 Future Design Considerations 20

References 21

1. Introduction

Might move below to abstract.

At CERN, a new electron cooler is being commissioned for the AD experiment. This cooler shoots electrons into ion-beam path. These electrons then collide with the beam particles, and momentum is transferred from the beam particles to the electrons. The electrons are then steered away from the beam path, into an electron collector.

In the beam path drift of the cooler, a solenoid magnet is used to orient the electron path. This magnet comes with strict requirements on field quality, in the order of $\vec{B}_{\perp}/\vec{B}_{\parallel} < 10\text{E}{-}10$. A new measurement system for solenoids has been proposed, using coils wound on a pcb. This pcb is then translated through the solenoid aperture, to obtain maps of the magnetic field. In this thesis, the metrological characterization of this system is presented, along with some post processing methods.

1.1 Project Purpose and Goal

1.2 Previous Work

2. Background

2.1 Electromagnetic Fields

The electromagnetic fields are a collection of closely linked fields. These fields govern the electric and magnetic interactions of charged particles and domains. These fields can be seen in table 2.1

Field	SI unit	Description
$\mathbf{H}$	$1\,Am^{-1}$	Magnetic Field
$\mathbf{E}$	$1\,Vm^{-1}$	Electric Field
$\mathbf{B}$	$1\,Vsm^{-2}$	Magnetic Flux Density
$\mathbf{D}$	$1\,Asm^{-2}$	Electric Flux Density
$\mathbf{J}$	$1\,Am^{-2}$	Electric Current Density
ρ	$1\,Asm^{-3}$	Electric Charge Density

These fields are described by Maxwells Equations. In differential form for the stationary case, these are as follows:

$$\nabla \times \mathbf{H} = \mathbf{J} + \frac{\partial}{\partial t}\mathbf{D} \tag{2.1}$$

$$\nabla \times \mathbf{E} = -\frac{\partial}{\partial t}\mathbf{B} \tag{2.2}$$

$$\nabla \cdot \mathbf{B} = \mathbf{0} \tag{2.3}$$

$$\nabla \cdot \mathbf{D} = \rho \tag{2.4}$$

Since we're dealing with measurement of magnetic fields in this thesis, equations 2.1 and 2.3 will naturally be of the most interest. In simple cases, the $\mathbf{H}, \mathbf{D}, \mathbf{E}$ and $\mathbf{B}$ field obey the easy relations

$$\mathbf{B} = \mu\mathbf{H} \tag{2.5}$$

$$\mathbf{D} = \varepsilon\mathbf{E} \tag{2.6}$$

where μ is the *magnetic permeability* and U is the *electric permittivity* in the domain of interest. Formally, simple cases are where the fields are located in a medium that is linear, homogenous across its domain, invariant depending on

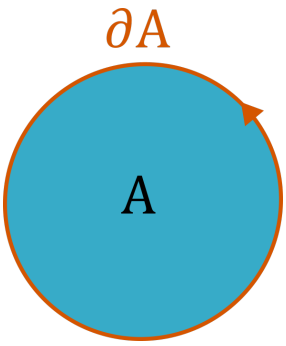

(a) An area A and its boundary ∂A.

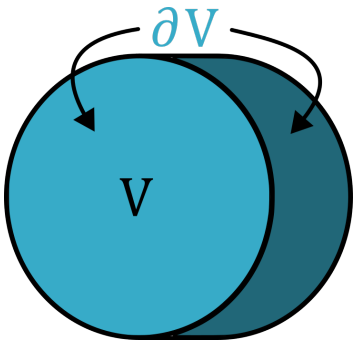

(b) A volume V and its surface boundary ∂V.

direction, and stationary. Since the magnetic measurements are made inside the empty aperture of the magnet, the domain is only made up of air. Thus, equation 2.5 holds, and the magnetic permeability is the one of free space, that is $\mu = \mu_0 = 4\pi \times 10^{-7} Hm^{-1}$. [3, Ch.4.1-4.4]

2.1.1 Magnetic Flux and Induction

Magnetic flux Φ is the surface integral of the **B** field along the normal vector to the surface. Mathematically, it is defined as:

$$\Phi(\mathrm{A}) = \iint_{\mathrm{A}} \mathbf{B} \cdot \hat{\mathbf{n}} \, d\mathrm{A} \tag{2.7}$$

where A is the surface, and $\hat{\mathbf{n}}$ is the normal vector to the surface. We then have the following governing laws of electromagnetism for objects at rest:

$$U(\partial \mathrm{A}) = -\frac{d}{dt}\Phi(\mathrm{A}) \tag{2.8}$$

$$\Phi(\partial \mathrm{V}) = 0 \tag{2.9}$$

Equation 2.8, also called faradays law, describes the voltage ε induced in a length of wire ∂A, enclosing an area A, when the magnetic flux Φ is changing with respect to time. The signs of U and Φ obey the right hand rule as indicated in figure 2.1a.

Equation 2.9 states that the total amount of flux flowing through the boundary ∂V of the volume V must equal 0.[3, Ch.4.1.1]

2.2 Series decompositions of the magnetic field

The magnetic field can be calculated in some different ways, for instance directly from Maxwells equations or using Biot-Savarts law:

$$\mathbf{B}(\mathbf{r}) = \frac{\mu_0}{4\pi} \int_{\mathrm{V}} \frac{\mathbf{J}(\mathbf{r}') \times (\mathbf{r} - \mathbf{r}')}{|\mathbf{r} - \mathbf{r}'|^3} d\mathrm{V} \tag{2.10}$$

where $\mathbf{B}(\mathbf{r})$ is the $\mathbf{B}$ field at coordinate $\mathbf{r}$ and $\mathbf{J}(\mathbf{r}')$ is the current distribution at coordinate $\mathbf{r}'$. [3, Ch.5.4] Except for very simple geometries, the magnetic field is rarely expressible using elementary functions. A common method is then to express it using fourier series solutions inside a specified domain. [3, Ch.6]

Inside the aperture of a magnet, the domain is free of currents and made up of air or vacuum. The current powering the magnet is constant, meaning we have a constant electric field. Equation 2.1 can then be rewritten as follows:

$$\begin{aligned} \nabla \times \mathbf{H} &= \mu_0 \nabla \times \mathbf{B} \\ \mu_0 \nabla \times \mathbf{B} &= \mathbf{J} + \frac{\partial}{\partial t}\mathbf{D}\Big|_{\substack{\mathbf{J}=\mathbf{0} \\ \frac{\partial}{\partial t}\mathbf{D}=\mathbf{0}}} \\ &= \mathbf{0} \end{aligned} \tag{2.11}$$

This, along with equation 2.3 means that there exists a magnetic scalar potential $\Psi(\mathbf{r})$ of $\mathbf{B}$ that satisfies Laplace's equation

$$\nabla^2 \Psi = \frac{\partial^2 \Psi}{\partial x^2} + \frac{\partial^2 \Psi}{\partial y^2} + \frac{\partial^2 \Psi}{\partial z^2} = 0 \tag{2.12}$$

inside the domain, where the $\mathbf{B}$ field components are

$$B_x = \frac{\partial \Psi}{\partial x}, B_y = \frac{\partial \Psi}{\partial y}, B_z = \frac{\partial \Psi}{\partial z} \tag{2.13}$$

2.2.1 Cylindrical Coordinates

Since the aperture of our magnet is cylindrical, working in cylindrical coordinates (r, φ, z) is a natural choice. They are related to the cartesian system (x, y, z) through the relations:

$$\begin{aligned} x &= r\cos\varphi \\ y &= r\sin\varphi \\ z &= z \end{aligned} \tag{2.14}$$

A vector $\mathbf{v}$ is defined by its distance r from the origin, its angle φ from the x-axis, and its offset in z as $\mathbf{v}(r,\varphi,z) = (r\cos\varphi, r\sin\varphi, z)$. Where in cartesian coordinates we have the basis vectors $\hat{\mathbf{e}}_\mathbf{x}, \hat{\mathbf{e}}_\mathbf{y}, \hat{\mathbf{e}}_\mathbf{z}$ along the x, y and z axis, in cylindrical coordinates we have $\hat{\mathbf{e}}_\mathbf{r}, \hat{\mathbf{e}}_\varphi, \hat{\mathbf{e}}_\mathbf{z}$ as illustrated in figure 2.2. Note that $\hat{\mathbf{e}}_\mathbf{r}$ and $\hat{\mathbf{e}}_\varphi$ change direction depending on the current value of φ.

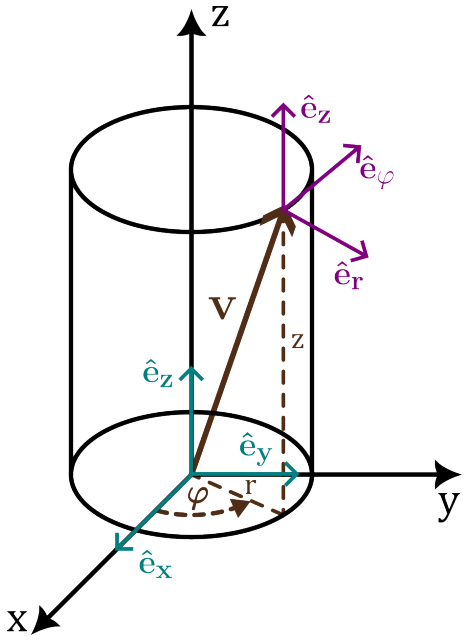

Figure 2.2. Cylindrical coordinates and their relationship to cartesian coordinates.

Scaling Factors

In cylindrical coordinates, scaling factors are needed for common differential operators. For a scalar field $\Psi(r,\varphi,z)$ the gradient is defined as

$$\nabla\Psi = \frac{\partial\Psi}{\partial r}\hat{\mathbf{e}}_\mathbf{r} + \frac{1}{r}\frac{\partial\Psi}{\partial\varphi}\hat{\mathbf{e}}_\varphi + \frac{\partial\Psi}{\partial z}\hat{\mathbf{e}}_\mathbf{z} \tag{2.15}$$

The divergence of a vector field $\mathbf{V}(r,\varphi,z)$ is

$$\nabla\cdot\mathbf{V} = \frac{1}{r}\frac{\partial}{\partial r}(rV_r) + \frac{1}{r}\frac{\partial V_\varphi}{\partial\varphi} + \frac{\partial V_z}{\partial z} \tag{2.16}$$

which gives the laplacian $\nabla^2\Psi = \nabla\cdot\nabla\Psi(r,\varphi,z)$

$$\nabla^2\Psi = \frac{1}{r}\frac{\partial}{\partial r}\left(r\frac{\partial\Psi}{\partial}\right) + \frac{1}{r^2}\frac{\partial^2\Psi}{\partial\varphi^2} + \frac{\partial^2\Psi}{\partial z^2} \tag{2.17}$$

[3, Ch.3.13]

The Laplace Equation in Cylindrical Coordinates

One way to solve the laplacian is to use separation of variables technique to find the set of potential solutions, and from that set choose the ones that make sense for our problem.

Firstly, we make the ansatz that the solutions can be written in the form

$$\Psi(r,\varphi,z) = R(r)\Phi(\varphi)Z(z) \tag{2.18}$$

Insertion of equation 2.18 into 2.17 then gives us

$$\nabla^2\Psi = \frac{1}{rR}\frac{d}{dr}\left(\frac{dR}{dr}\right) + \frac{1}{r^2\Phi}\frac{d^2\Phi}{d\varphi^2} + \frac{1}{Z}\frac{d^2Z}{dz^2} \tag{2.19}$$

We know from equation 2.12 that this is equal to zero, and can therefore rewrite as

$$-\frac{1}{\Phi}\frac{d^2\Phi}{d\varphi^2} = \frac{r}{R}\frac{d}{dr}\left(\frac{dR}{dr}\right) + \frac{r^2}{Z}\frac{d^2Z}{dz^2} \tag{2.20}$$

Here, a contradiction emerges. A change in φ can only introduce a change in the left hand side of this equation. Likewise, this equality must still hold for a change in r or z. These conditions only hold under the assumption that both sides are constant, such that

$$\frac{1}{\Phi}\frac{d^2\Phi}{d\varphi^2} = \alpha_1 \tag{2.21}$$

where α_1 is constant. Using similar reasoning for $Z(z)$ and then $R(r)$ we can reduce this partial differential equation to a system of ordinary differential equations.

$$\frac{d^2R}{dr^2} + \frac{1}{r}\frac{dR}{dr} = \left(\frac{\alpha_1}{r^2} + \alpha_2\right)R \tag{2.22}$$

$$\frac{d^2\Phi}{d\varphi^2} = \alpha_1\Phi \tag{2.23}$$

$$\frac{d^2Z}{dz^2} = \alpha_2 Z \tag{2.24}$$

While the differential equations in Φ and Z have a well defined set of solutions using elementary functions like sines, cosines and exponentials, equation 2.22 is a bit trickier. This equation is known as the Bessel differential equation, and solving it will require a set of functions known as the Bessel functions.

2.2.2 Bessel Functions

The Bessel functions are defined as the solutions to equation 2.22. They come in several different variants depending on the values of α_1 and α_2. They are not expressible using elementary functions and are therefore often approximated using power series solutions, generating functions or numeric integration.

The actual calculation of the Bessel functions is outside the scope of this thesis, more than stating that they are implemented in most popular programming languages. Still, a short overview of the properties of the most relevant subset of Bessel functions will aid greatly in finding the solutions to our magnetic scalar potential. [4]

Bessel Function, First Kind

The Bessel function of the first kind is a collection of functions that are non-singular at the origin. It is often denoted $J_n(x)$. Figure 2.3 shows $J_n(x)$ for $n = 0, 1, 2, 3, 4$.[5]

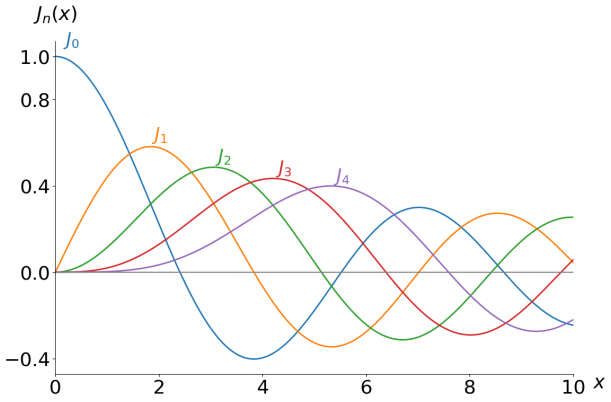

Figure 2.3. Bessel functions of the first kind, for $n \in [0,4]$.

For negative n we have

$$J_{-n}(x) = (-1)^n J_n(x) \tag{2.25}$$

Modified Bessel Function, First Kind

For the bessel function of the first kind with imaginary arguments, the modified Bessel function $I_n(x)$ is often used. It is related to the regular first kind Bessel function through the equality

$$I_n(x) = j^{-n} J_n(jx) \tag{2.26}$$

[7] The first five terms of I_n can be seen in figure 2.4.

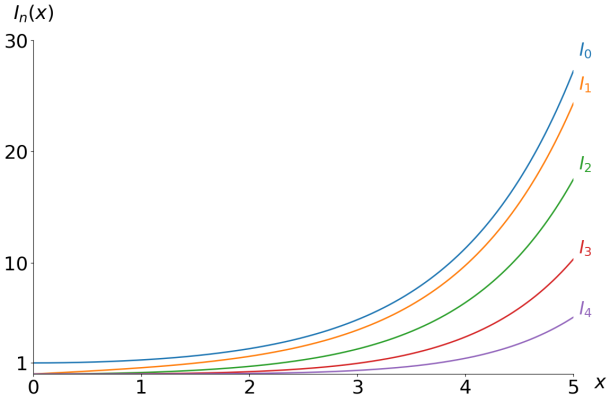

Figure 2.4. Modified Bessel functions of the first kind, for $n \in [0,4]$.

Bessel Function, Second Kind

The bessel function of the second kind is a solution to the bessel differential equation that is singular at the origin. It can be seen in figure 2.5.[6]

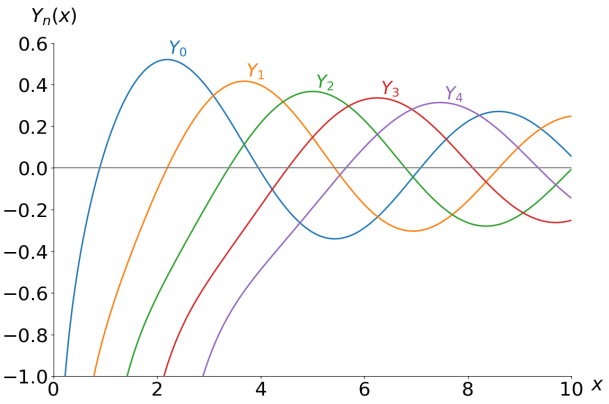

Figure 2.5. Bessel functions of the second kind, for $n \in [0,4]$.

2.2.3 Bessel-Fourier-Fourier Series

With the set of potential solutions to $\Psi(r,\varphi,z)$ established, we can start to eliminate the impossible ones. The domain Ω is spanned by the magnetometer and its path along the z axis, making up the cylindrical domain. Examples of this domain can be seen in figures 2.6a and 2.6b. Keep in mind that the domain is always spanned by and relative to the magnetometer and its path along z, and is thus the same regardless of the magnets relative positioning to the PCB. Using a table of known solutions to equations 2.22-2.24 from the book "Field

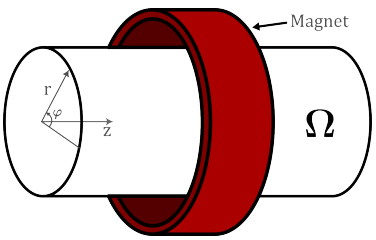

(a) The measurement domain Ω inside the aperture of a solenoid.

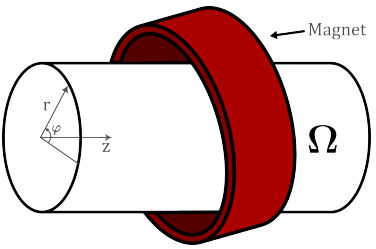

(b) The measurement domain Ω inside the aperture of an unaligned solenoid.

theory handbook" [2] we can find the relevant ones.

$$\frac{d^2R}{dr^2} + \frac{1}{r}\frac{dR}{dr} = \left(\frac{\alpha_1}{r^2} + \alpha_2\right) R \qquad \text{(2.22 revisited)}$$

$$\frac{d^2\Phi}{d\varphi^2} = \alpha_1 \Phi \qquad \text{(2.23 revisited)}$$

$$\frac{d^2Z}{dz^2} = \alpha_2 Z \qquad \text{(2.24 revisited)}$$

Firstly, the measurements start and end far outside of the magnet, where the field is very close to zero. Thus, the sum of the solutions in z must start and end at zero. Since the solutions must be periodic over the length of the domain, we have our first boundary condition

$$qkz = \frac{2\pi}{L}kz,\ k \in \mathbb{N}_1 \tag{2.27}$$

$$Z(z) = 0 \text{ if } z \in \{0, L\} \tag{2.28}$$

where $-(qk)^2 = \alpha_2$ and L is the length of the domain in z.

A Fourier series is then an appropriate solution.

$$Z(z) = \sum_{k=1}^{\infty} A_{zk}\sin(qkz) + B_{zk}\cos(qkz) \tag{2.29}$$

where A_{zk}, B_{zk} are as of yet unknown coefficients.

Secondly, since $\Phi(\varphi)$ spans the whole circumference of Ω, and the field is continuous inside the domain, we have our next boundary condition

$$\Phi(0) = \Phi(2\pi) \tag{2.30}$$

Once again, a Fourier series is an appropriate solution

$$\Phi(\varphi) = \sum_{n=1}^{\infty} A_{\varphi n}\sin(n\varphi) + B_{\varphi n}\cos(n\varphi),\ n \in \mathbb{N}_1 \tag{2.31}$$

giving us $\alpha_1 = -n^2$.

With both α_1 and α_2 found, $R(r)$ in equation 2.22 is now completely determined as

$$R(r) = \sum_{k=0}^{\infty} A_{rk}J_k(jqkr) + B_{rk}Y_k(jqkr) \tag{2.32}$$

Since we know that the magnetic field is not singular inside the aperture (Biot Savart, equation 2.10 gives us singularities only inside the current carrying wires.) we can immediately discard Y_k as potential solution. Since the argument for J_k is imaginary, we can also substitute with the modified Bessel function of the first kind, giving us

$$R(r) = \sum_{k=1}^{\infty} j^{-k}A_{rk}I_k(qkr) \tag{2.33}$$

We still need to account for the fact that the **B**-field might have a non zero mean over the domain, i.e. adding the zero terms of the series. For $Z(z)$, this is simply

$$Z(z) = A_{z0}z \tag{2.34}$$

while in r this will be

$$R(r) = \sum_{n=1}^{\infty} A_{r0}r^n \tag{2.35}$$

[2, pp.12-14] The $n = 0$ terms for $R(r)$ and $\Phi(\varphi)$ have been discarded, as that would be equivalent to a magnetic monopole, which have never been found experimentally, and is unlikely to be found using a simple solenoid magnet.[1]

Now, all the potential solutions can be combined into one double series. By also converting the Fourier series from real to complex valued double sided series, we can combine the $A_{n,k}$ and $B_{n,k}$ coefficients into one complex valued coefficient $\mathfrak{C}_{nk}$. The values of these coefficients are unknown until fitted to measurements.

After a lot of algebra, this yields

$$\begin{aligned}\Psi(r,\varphi,z) = \mathfrak{C}_{0,0}z + \frac{1}{2}\sum_{\substack{k=-\infty\\k\neq 0}}^{\infty} \mathfrak{C}_{0,k}I_0\left(\frac{2\pi}{L}|k|r\right)\exp\left(j\frac{2\pi}{L}kz\right) + \\ + \frac{1}{2}\sum_{\substack{n=-\infty\\n\neq 0}}^{\infty} \mathfrak{C}_{n,0}r^{|n|}\exp(jn\varphi) + \\ + \frac{1}{4}\sum_{\substack{n=-\infty\\n\neq 0}}^{\infty}\sum_{\substack{k=-\infty\\k\neq 0}}^{\infty} \mathfrak{C}_{n,k}j^{-|n|}I_{|n|}\left(\frac{2\pi}{L}|k|r\right)\exp\left(j\frac{2\pi}{L}kz\right)\exp(jn\varphi)\end{aligned} \tag{2.36}$$

Technically, summands 1,2 and 4 can be merged into one sum, they are however separated to make the distinction of the fundamental fourier series in z and the higher order harmonics clearer.

It is worth noting that the third summand in the above series are a commonly used form of two dimensional multipoles at CERN. These are mainly used for dipole, quadropole, sextupole and higher order magnets with no or very little B-field derivative along the z axis inside the aperture. [3, Ch.6.1]

2.2.4 Fundamentals and Harmonics of the BFF Series.

As stated at the end of section 2.2, the **B** field components can be found by taking the partial derivatives of our scalar potential in equation 2.36. Since we will in actuality not be using an infinite amount of terms for our series, the

notation $\hat{\mathbf{B}}$ will be used for our estimated $\mathbf{B}$ field. The B_z component will then be

$$\hat{B}_z = \frac{\partial \Psi}{\partial z} = \mathfrak{C}_{0,0} + \frac{1}{2}\sum_{\substack{k=-\infty \\ k\neq 0}}^{\infty} \mathfrak{C}_{0,k} j\frac{2\pi}{L} k I_0\left(\frac{2\pi}{L}|k|r\right)\exp\left(j\frac{2\pi}{L}kz\right) + \\ + \frac{1}{4}\sum_{\substack{n=-\infty \\ n\neq 0}}^{\infty}\sum_{\substack{k=-\infty \\ k\neq 0}}^{\infty} \mathfrak{C}_{n,k} j^{-|n|+1}\frac{2\pi}{L} k I_{|n|}\left(\frac{2\pi}{L}|k|r\right)\exp\left(j\frac{2\pi}{L}kz\right)\exp(jn\varphi) \tag{2.37}$$

while in r we have

$$\hat{B}_r = \frac{\partial \Psi}{\partial r} = \frac{1}{2}\sum_{\substack{k=-\infty \\ k\neq 0}}^{\infty} \mathfrak{C}_{0,k}\frac{2\pi}{L}|k| I_0'\left(\frac{2\pi}{L}|k|r\right)\exp\left(j\frac{2\pi}{L}kz\right) + \\ + \frac{1}{2}\sum_{\substack{n=-\infty \\ n\neq 0}}^{\infty} \mathfrak{C}_{n,0}|n| r^{|n|-1}\exp(jn\varphi) \\ + \frac{1}{4}\sum_{\substack{n=-\infty \\ n\neq 0}}^{\infty}\sum_{\substack{k=-\infty \\ k\neq 0}}^{\infty} \mathfrak{C}_{n,k}\frac{2\pi}{L}|k| j^{-|n|} I_{|n|}'\left(\frac{2\pi}{L}|k|r\right)\exp\left(j\frac{2\pi}{L}kz\right)\exp(jn\varphi) \tag{2.38}$$

and finally, in φ

$$\hat{B}_\varphi = \frac{1}{r}\frac{\partial \Psi}{\partial \varphi} = \frac{1}{2}\sum_{\substack{n=-\infty \\ n\neq 0}}^{\infty} \mathfrak{C}_{n,0} jn r^{|n|-1}\exp(jn\varphi) + \\ + \frac{1}{4}\sum_{\substack{n=-\infty \\ n\neq 0}}^{\infty}\sum_{\substack{k=-\infty \\ k\neq 0}}^{\infty} \mathfrak{C}_{n,k}\frac{n}{r} j^{-|n|+1} I_{|n|}\left(\frac{2\pi}{L}|k|r\right)\exp\left(j\frac{2\pi}{L}kz\right)\exp(jn\varphi) \tag{2.39}$$

We will now study the individual harmonics of the BFF series. Using numerical calculations from a simple current loop Biot-Savart model, the BFF series was fitted to $\mathbf{B}$ field points inside a cylindrical domain.

2.3 Signal Processing

2.3.1 Filters

2.3.2 Least Squares Fitting

3. The Translating Coil Magnetometer

3.1 PCB printed coils
3.2 Positional Encoder
3.3 Geometric Lidar Measurements
3.4 Fast Digital Integrators
3.5 The Measurement Assembly

4. Measurements

4.1 Solenoidal Field Maps

4.2 The Magnet-Magnetometer Yaw Angle Peak Shift

5. Post Processing

5.1 Lidar Scans

5.2 Coil Induction Analysis

5.3 Bessel-Fourier-Fourier Series Fitting

5.4 Estimating the Magnet-Magnetometer Yaw Angle

6. Discussion

6.1 Metrological Characterization

6.2 Future Design Considerations

References

[1] B. Acharya, J. Alexandre, P. Benes, B. Bergmann, S. Bertolucci, A. Bevan, H. Branzas, P. Burian, M. Campbell, Y. M. Cho, M. de Montigny, A. De Roeck, J. R. Ellis, M. El Sawy, M. Fairbairn, D. Felea, M. Frank, O. Gould, J. Hays, A. M. Hirt, D. L.-J. Ho, P. Q. Hung, J. Janecek, M. Kalliokoski, A. Korzenev, D. H. Lacarrère, C. Leroy, G. Levi, A. Lionti, A. Maulik, A. Margiotta, N. Mauri, N. E. Mavromatos, P. Mermod, L. Millward, V. A. Mitsou, I. Ostrovskiy, P.-P. Ouimet, J. Papavassiliou, B. Parker, L. Patrizii, G. E. Păvălaş, J. L. Pinfold, L. A. Popa, V. Popa, M. Pozzato, S. Pospisil, A. Rajantie, R. Ruiz de Austri, Z. Sahnoun, M. Sakellariadou, A. Santra, S. Sarkar, G. Semenoff, A. Shaa, G. Sirri, K. Sliwa, R. Soluk, M. Spurio, M. Staelens, M. Suk, M. Tenti, V. Togo, J. A. Tuszyn'ski, A. Upreti, V. Vento, and O. Vives. Search for magnetic monopoles produced via the schwinger mechanism. *Nature*, 602(7895):63–67, February 2022.

[2] Parry Hiram Moon and D E Spencer. *Field theory handbook*. Springer, Berlin, Germany, 2 edition, May 1988.

[3] Stephan Russenschuck. *Field computation for accelerator magnets: analytical and numerical methods for electromagnetic design and optimization*. John Wiley & Sons, 2011.

[4] Eric W. Weisstein. Bessel Function – from Wolfram MathWorld. `https://mathworld.wolfram.com/BesselFunction.html`.

[5] Eric W. Weisstein. Bessel Function of the First Kind – from Wolfram MathWorld.

[6] Eric W. Weisstein. Bessel Function of the Second Kind – from Wolfram MathWorld.

[7] Eric W. Weisstein. Modified Bessel Function of the First Kind – from Wolfram MathWorld.